ISSN 1995-0780, Nanotechnologies in Russia, 2017, Vol. 12, Nos. 1–2, pp. 49–61. © Pleiades Publishing, Ltd., 2017.
Original Russian Text © E.K. Papynov, O.O. Shichalin, V.Yu. Mayorov, E.B. Modin, A.S. Portnyagin, I.A. Tkachenko, A.A. Belov, E.A. Gridasova, I.G. Tananaev, V.A. Avramenko, 2017, published in Rossiiskie Nanotekhnologii, 2017, Vol. 12, Nos. 1–2.

Spark Plasma Sintering as a High-Tech Approach in a New Generation of Synthesis of Nanostructured Functional Ceramics

E. K. Papynov[a,b]*, O. O. Shichalin[a,b], V. Yu. Mayorov[a], E. B. Modin[b,c], A. S. Portnyagin[a,b], I. A. Tkachenko[a], A. A. Belov[b], E. A. Gridasova[b], I. G. Tananaev[a,b], and V. A. Avramenko[a,b]

[a] *Institute of Chemistry, Far East Branch, Russian Academy of Sciences, Vladivostok, 690022 Russia*
[b] *Far Eastern Federal University, Vladivostok, 690091 Russia*
[c] *National Research Center "Kurchatov Institute", Moscow, 123098 Russia*
**e-mail: papynov@mail.ru*

Received September 29, 2016; in final form, October 13, 2016

Abstract—The results of Spark Plasma Sintering (SPS) synthesis of different types of ceramic materials for various industrial applications are presented. A high quality of ceramics is achieved through the originality of the developed approach based on combining SPS technology with other methods of inorganic synthesis, for instance, with sol–gel technology. The suggested approach enables one to synthesize, at the first stage, nanostructured powders of inorganic materials, whose subsequent consolidation by the SPS method ensures the formation of nanostructured ceramics with unique physicochemical characteristics and properties.

DOI: 10.1134/S1995078017010086

The earlier unstudied magnetic ceramics based on individual α-Fe_2O_3 (hematite) and an α-Fe_2O_3–Fe_3O_4 composite (hematite–magnetite) with a porous structure of high construction strength (crush strength at least 249 MPa) extensively applied in electrical engineering have been synthesized using the suggested approach. It has been demonstrated for the first time that SPS technology allows the formation of highly magnetic ceramic composites based on antiferromagnetic hematite powders upon their high-temperature sintering: the magnetization value (Ms) increases at least tenfold.

Novel bioceramics with bimodal pore size distribution (100–500 nm and 1–500 μm) and high construction strength (from 72.5 up to 172 MPa), which are similar to the bone tisue texture and, therefore, have good prospects in practical medicine, have been synthesized on the basis of nanostructured wollastonite. Using the present study, the peculiarities of formation of a biporous silicate framework have been studied under in situ conditions for the first time. Two types of pore-forming additives (templates) of different natures, shapes, and sizes were introduced at different stages of sol–gel and SPS syntheses: organic–inorganic (polymer latex of the "core–shell" type) and inorganic (carbon filler). The effect of the carbon template content (5 or 25 wt %) on structural and strength parameters of the wollastonite ceramics synthesized in spark plasma current is described.

The prospects of applying SPS technology to create high-density glass ceramics for the immobilization of hazardous radionuclides (nuclear ceramics) have been demonstrated. In particular, zeolite–ceramics matrices with immobilized cesium (cesium mass fraction ~20%) characterized with low leachability with respect to cesium ($<10^{-6}$–10^{-7} g/cm^2 day) and high mechanical strength (up to 500 MPa) are fabricated. The results of studies prove the expediency of applying SPS technology in nuclear industry: first, in creating compact compounds containing hazardous radionuclides (for example, spent sorbents saturated with radioactive cesium) suitable for long-term and safe storage and, second, in manufacturing radioisotope products—sources of ionizing radiation containing zeolite glass ceramics with immobilized radionuclides in precise specific activity doses as an active base (filler).

INTRODUCTION

One of the tasks of advanced materials science is to search for new routes of producing ceramic materials. In this regard, much interest of researchers is concerned with unique properties of ceramics, whose specific combinations in a single material inevitably develop new practical applications. However, to produce functional ceramics, it is necessary to control the size and spatial orientation of the resulting material grain without loss of the possibility of controlling chemical and phase composition, as well as physical characteristics.

In view of the above, a promising solution consists of the application of advanced technologies of powder metallurgy, in particular, Spark Plasma Sintering (SPS), also known in Russia as Electric Pulse Sintering under Pressure (EPSP) [1]. The main SPS feature comprises high-rate sintering of powder materials with the formation of ceramics of a new type characterized with unique compositions and properties. Such materials include biomaterials and functional-gradient, thermoelectric, hard-alloy, nuclear, optical, and composite materials, as well as metal alloys and many others [2, 3]. SPS technology provides the fabrication of ultra-advanced ceramics that do not have worldwide analogs (a product of the 21st century) and are in a great demand in all fields of industry.

The uniqueness of the SPS technology consists of the mechanism of the sintering process, in particular, in heating conditions. The process is based on the principle of powder consolidation in the direct-current electric field under the effect of high-energy low-voltage pulses (power up to 100 kJ, periodicity from 3.3 to 326.7 ms, and frequency of 50 Hz) and constant mechanical load (in the range from 0 to 30 t). Pulses generate spark discharges between the particles of the material to be sintered, thus concentrating, in respective sites, large amounts of thermal energy (Joule heat) and locally heating powder particles up to temperatures from a few to tens of thousands of degrees Celsius within fractions of seconds. This results in partial melting or evaporation of the material; its thermal and electrolytic diffusion; and, finally, sintering [1–5].

The key difference between SPS technology and conventional powder metallurgy methods is that sintering of powder particles is achieved at the expense of internal thermal of the material. This is different from other sintering types, in which the necessary Joule effect energy is provided to the material from outside (inductive or resistive heater), which requires hours-long holding [6]. Prolonged treatment in conventional methods is related to the fact that for this type of heat transfer between the workpiece core and periphery (surface) there is a significant temperature gradient (spatial temperature heterogeneity), especially for bulky parts, which can be excluded only through this very treatment duration. Also, imposing an external pressure required to impart necessary strength to the compound is possible only after a certain period (when workpiece temperature becomes leveled over the whole volume). In case of the SPS technology, the above problems are eliminated, since heating by pulse current has a number of advantages: first, it provides high heating rates (up to 200°C/min) and short duration of the sample holding at the final consolidation temperature (a few minutes), which facilitates the removal of impurities from the particle surface (surface cleaning and activation); second, is limits the grain growth (minimal changes); and, third, it preserves the real microstructure of the final sample (controlled porosity), so that the real sintering temperature is lower than the theoretical one (by 1/3 on average). Here, the electric current of the pulse type creates conditions for homogeneous heat distribution over the sample, also independently of the nature of the powder material to be sintered (conductors or dielectrics), which allows the fabrication of multicomponent composites. In addition, the fabricated material density may attain the maximal one ("full" density, up to 99.9% of the theoretical one), when the materials will be characterized with high homogeneity and especially strong bonds between particles [1–5]. The targeted pulse currents also have an orienting effect on magnetic moments of atoms and ions in crystallites, thus promoting the formation of magnetic properties in materials [7]. The SPS technology makes it possible to produce a machine part immediately in the final form and obtain a profile of the workpiece close to the required one.

The universal character of the described approach consisting of the possibility of producing a large class of advanced ceramics for various practical purposes reflects the objective of the present study, which has been demonstrated in the present work on the example of SPS synthesis of magnetic ceramics necessary for electrical engineering, bioceramics that are in high demand for practical medicine, and nuclear ceramics as a promising solution in the fields of radioecology and manufacture of innovative radioisotope products for nuclear industry.

EXPERIMENTAL

Synthesis of Magnetic Ceramics

For the magnetic ceramics synthesis, the finely dispersed powder of nanostructured hematite (α-Fe_2O_3) (fraction 0.1–0.5 mm) of the macroporous structure (pore size 100–500 nm) obtained through template sol–gel synthesis according to the technique described in [8] was used.

Consolidation of the hematite powder with producing a ceramic compound was carried out using an SPS-515S device manufactured by Dr. Sinter Lab (Japan) in accordance with the following scheme: 3 g of the initial finely dispersed hematite powder was placed into a graphite mold (diameter 15 mm) and compacted (pressure 20.7 MPa), after which the workpiece was placed into a vacuum chamber (pressure 6 Pa) and sintered. A series of several samples was fabricated in several experiments carried out at different sintering temperatures of 700, 800, 900, 1000, and 1100°C; a constant load of 24.5 MPa; a heating rate of 170°C/min; and a holding period of 5 min (Table 1).

Synthesis of Bioceramics

Precursors: sodium metasilicate ($Na_2SiO_3 \cdot 5H_2O$, chemically pure grade) and calcium chloride ($CaCl_2 \cdot 2H_2O$, pure grade). The commercially available siloxane–acrylate emulsion KE 13–36 [9] (solid phase content 50%; particle size 160 nm) manufactured by

Table 1. Characteristics of ceramic samples fabricated by SPS synthesis of nanostructured hematite

No.	T_s, °C	XRD	S_{spec} (BET), m^2/g	Fracture strength, MPa	M, emu/g	H, Oe
					300 K	300 K
1	Initial	Hematite (α-Fe_2O_3)	6.2	–	0.8	1260
2	700	Hematite (α -Fe_2O_3)	7.5	31	1.2	1130
3	800	Hematite (α-Fe_2O_3) Carbon (C)	4.2	243	2.5	1070
4	900	Hematite (α-Fe_2O_3) Carbon (C)	0.7	249	3.6	990
5	1000	Hematite (α-Fe_2O_3) Magnetite (Fe_3O_4) Carbon (C)	0.1	249	4.8	140
6	1100	Hematite (α-Fe_2O_3) Magnetite (Fe_3O_4) Carbon (C)	0.1	249	10.2	60

JSC Astrokhim (Elektrostal', Moscow oblast), whose colloid properties were described in [10], and finely dispersed carbon of the technical grade (particle size 1–500 μm) were used as templates.

Fabrication of biporous ceramic wollastonite was carried out by two consecutive methods (general synthesis scheme is shown in Fig. 3):

1. Sol–gel synthesis of the composite material based on calcium hydrosilicate (xonotlite) using a colloid template (polymer latex).

Synthesis of the composite based on calcium hydrosilicate (xonotlite) mixed with a colloid template was carried out by the sol–gel method in accordance with the following scheme: 50 mL of a solution of the siloxane–acrylate emulsion (template) diluted by distilled water at a ratio of 1 : 10 was added, under constant stirring, with 50 mL of 1 N solution of calcium chloride and 50 mL of 1 N solution of sodium metasilicate. Upon stirring for 3 h at 100°C, the mixture was cooled down to room temperature (25°C), filtered through the blue ribbon filtering paper, washed with distilled water until negative reaction to chloride ions, and dried at 105°C.

2. SPS consolidation of the composite material based on the latex-containing xonotlite using an inorganic template (graphite).

Consolidation of the powder of a composite material based on the latex-containing xonotlite was carried out in the presence of a carbon template by the method of Spark Plasma Sintering using an SPS-515S device (Dr. Sinter Lab, Japan) in accordance with the following scheme: 3 g of the initial xonotlite (powder of the fraction 0.1–1 mm), also with addition of the carbon template in amounts of 5 and 25 wt % (graphite with the particle size in the range 1–500 μm), was placed into a graphite mold (diameter 15 mm) and compacted (pressure 20.7 MPa), after which the workpiece was placed into a vacuum chamber (pressure 6 Pa) and sintered. The sintering temperature was 900°C, the mechanical load was 24.5 MPa, the heating rate was 170°C/min, and the holding time was 5 min.

Removal of colloid and carbon templates was performed through the thermal oxidation treatment of consolidated samples at 900°C for 1 h with a heating rate of 5°C/min in a muffle furnace (Nabertherm GmbH, Germany).

Synthesis of Nuclear Ceramics

Natural zeolite (clinoptilolite) from the Chuguevka deposit (Chuguevka, Primorskii krai, Russia) characterized with the SiO_2/Al_2O_3 content ratio from 8.8 to 9.4 was used as the initial powder for sintering [11].

To saturate the natural zeolite of the Chuguevka deposit with cesium ions, the zeolite powder of specific fraction (50–100 μm) and solution of cesium nitrate with a Cs concentration of 5 g/L were prepared. For this purpose, the initial zeolite powder was sieved using microsieves of different grits (50–1000 μm) and the selected fraction (50–100 μm) was washed with distilled water to remove fine dust. Thereafter, zeolite was dried at 100°C until complete water removal.

To prepare a cesium solution with a cesium concentration of 5 g/L, 1.6745 g of cesium nitrate ($CsNO_3$) was dissolved in water in a graduated flask of a volume of 200 mL.

The prepared 10 g of zeolite was placed into 100 mL of solution with a Cs concentration of 5 g/L for 1 day until complete cesium adsorption from this solution, washed with distilled water, and dried at 100°C until constant weight.

Synthesis of ceramic matrices was carried out through the consolidation of the zeolite powder saturated with cesium in a flow of spark plasma using an SPS–515S device (Dr. Sinter Lab, Japan) in accordance with the following scheme: 3 g of the initial zeolite powder (fraction 50–100 μm) was placed into a

graphite mold (diameter 15 mm) and compacted (pressure 20.7 MPa), after which the workpiece was placed into a vacuum chamber (pressure 6 Pa) and sintered. The sintering temperature was varied in the range 700–1100°C, the mechanical load was 24.5 MPa, the heating rate was 140°C/min, and the holding time was 5 min.

The chemical stability of zeolite–ceramics matrices to cesium leaching was carried out under conditions of a prolonged contact with distilled water in compliance with the Russian State Standard (GOST) R 52126-2003. Determination of the cesium concentration in solution at leaching was carried out using a Thermo M Series atomic-absorption spectrometer (United States). Calculation and processing of test results were performed in compliance with the Russian State Standard (GOST) R 52126-2003:

$$R_n^i = m_n^i/(M_0^i S t_n),\ \text{g/(cm}^2\ \text{day)},$$

where m_n^i is the mass (g) of the i element leached within the n-interval of the t_n test duration (days), M_0^i is the mass concentration (g/g) of the i element in the matrix, and S is the areas of the sample open geometric surface, cm^2.

METHODS OF STUDY

Identification of phases of the fabricated samples was performed by X-ray diffraction analysis (XRD) (CuKα-radiation, Ni-filter, average wavelength (λ) 1.5418 Å, registered angles range 10–80°, scanning increment 0.02°, and spectra registration rate 5 deg/min) using a D8 Advance multipurpose X-ray diffractometer (Bruker AXS, Germany). Pore size distribution was determined using an AutoPore IV mercury porosimeter (Micromeritics, United States). Analysis of the surface area and porosity of solid bodies was performed by the method of physical adsorption using an ASAP 2020 device (Micromeritics, United States). Images of the structure of the materials under study were obtained by scanning electron microscopy (SEM) using S-3400N (Hitachi, Japan) and Dual Beam Carl Zeiss CrossBeam 1540 XB (Germany) devices. Magnetic characteristics were investigated using a SQUID magnetometer (Quantum Design, United States). Measurements of the specific density were performed by hydrostatic weighing using an Adventurer™ balance (OHAUS Corporation, United States). The mechanical compression strength for samples of cylindrical shapes (diameter 15 mm and height from 6 to 10 mm) was determined using an Autograph AG-X plus 50 kN tension testing machine (Shimadzu, Japan) at a load rate of 0.5 mm/min.

RESULTS AND DISCUSSION

Magnetic Ceramics

Among a great number of magnetic materials applied in different fields of industry, science, and technology, ceramic systems based on iron oxides occupy a special position [11]. Magnetic ceramics are used in most cases as an alternative to metallic magnets to reduce energy losses associated with remagnetization. Such a replacement is possible due to the high electric resistance of the oxide ceramics, in particular, ferrites (based on maghemite, magnetite, and, more rarely, hematite), and, as a result, a substantial reduction of vortex currents and related electromagnetic losses [11, 12]. However, the synthesis of magnetic ceramics poses a number of difficulties: in particular, their magnetic properties are structure-sensitive [13] and determined not only by the composite phase composition, but also by the crystallite size and shape and various heterogeneities. To sum up, of special importance is the method of synthesis, capable not only of effectively reducing the content of heterogeneities of various types, but also forming a specified material stoichiometry with chemical and structural homogeneity, thus increasing the product magnetic properties. The SPS technology is extensively used for this very purpose [7, 14]. Under its application conditions, the impact of the electromagnetic field promotes ordering of spatial positions of magnetic moments of metal ions in the material crystal lattice [15]. Here, the mechanical load in the course of sintering induces transformation of crystalline nanophases of iron oxides, transitions of the wüstite–magnetite–maghemite–hematite type, and, finally, the formation of new magnetic phases [16–18]. However, understanding all these mechanisms occurring in the spark plasma current upon the consolidation of magnetic powders (as was, for example, described for maghemite [19]) is insufficiently developed for most of the materials or (as in case of hematite) is completely absent.

In view of the above, we attempted to study the possibility of SPS synthesis of magnetic ceramics based on hematite (α-Fe_2O_3) in order to examine and characterize the behavior of magnetic properties of the antiferromagnet upon its electrophysical treatment. The nanostructured form of hematite obtained by sol–gel synthesis was used as its initial powder [8]. The idea of such an approach was based on possible formation of nanostructured ceramics produced by the developed porosity of the initial hematite powder. As a result, a series of magnetic ceramics samples with specific physical–chemical characteristics was synthesized at high temperatures of SPS synthesis in the range 700–1100°C (Table 1).

It has been revealed by the present study that the SPS process temperature affects all the parameters of the fabricated ceramics samples. High-temperature SPS modes activate solid-phase processes, resulting in irreversible reactions in the solid body: in particular, they are able to affect the stable crystalline form of hematite. The XRD data indicate that the crystalline phase of the initial α-Fe_2O_3 remains unchanged upon sintering at 700–900°C (Table 1), as in the case of low SPS temperature [20]. The hematite stability is disrupted upon heating above 1000°C, and the formed ceramic composites comprise a mixture of hematite

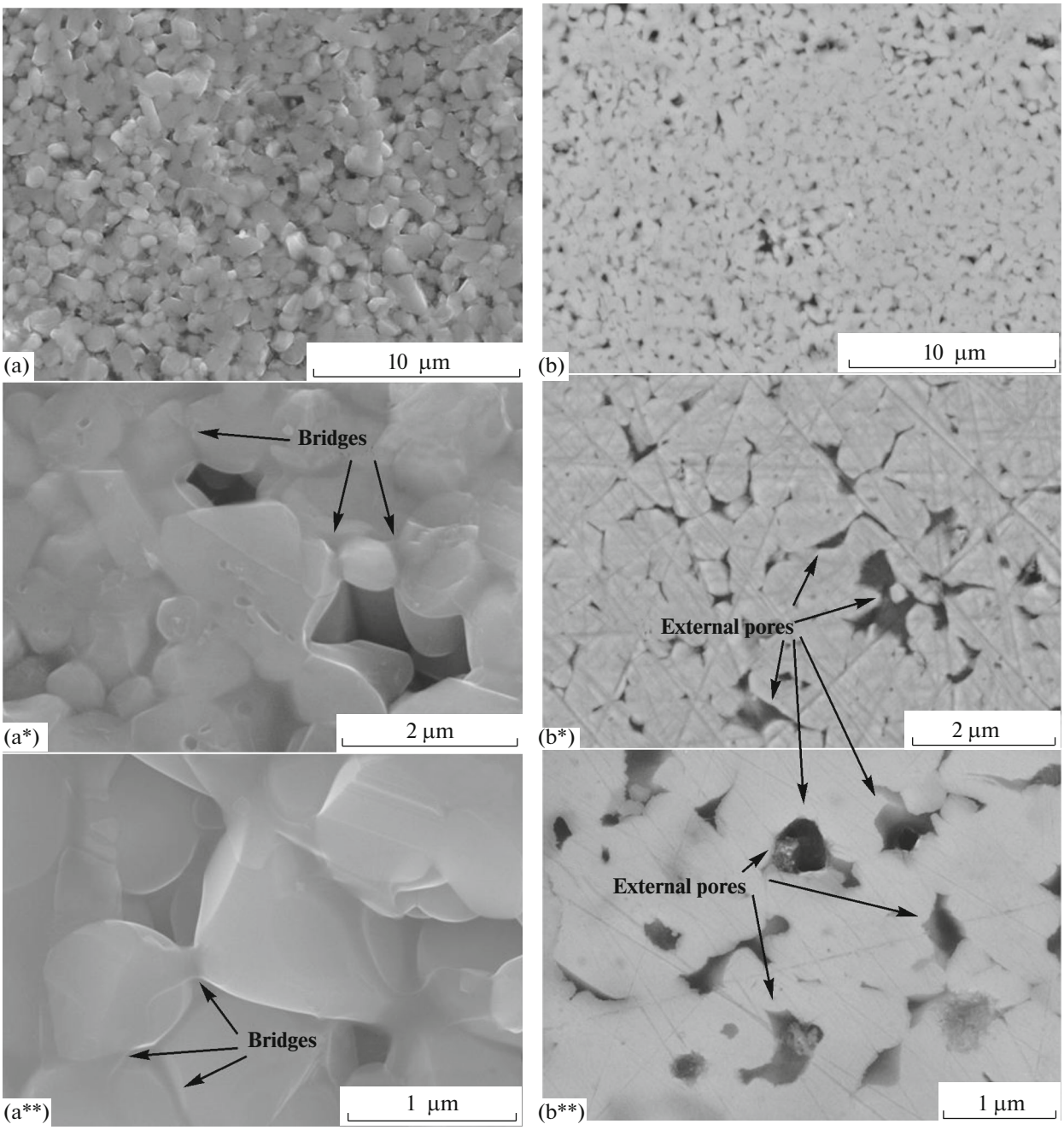

Fig. 1. Microstructure of the surface (a, a*, a**) and cross section (b, b*, b**) of the sample of magnetic ceramics fabricated by SPS at 900°C.

and magnetite (Table 1). However, the presence of a carbon (graphite) phase was detected in the composition of ceramic samples above 800°C. The emergence of free carbon in SPS composites was earlier reported by many researchers and is caused by its presence in the composition of electrodes, molds, insulating paper, and other process parts [21].

It was mentioned that the destruction of the porous structure of the materials occurred upon a temperature increase as a result of intensification of the process of diffusion and plastic deformation with attainment of the creep threshold and, finally, the material yielding flow. Here, the value of the material specific surface area decreases abruptly from 6.2 down to 0.1 m^2/g. However, the synthesized compounds become strengthened, and the modulus of elasticity increased from 31 up to 249 MPa (Table 1).

The effect of temperature on the surface morphology and the structure of bulk ceramics obtained in the spark plasma current was studied and shown in SEM images (Fig. 1). It was revealed that the destruction and reorientation of the initial powder particles, their dense compaction, and sintering along contact boundaries with formation of "necks" ("bridges")

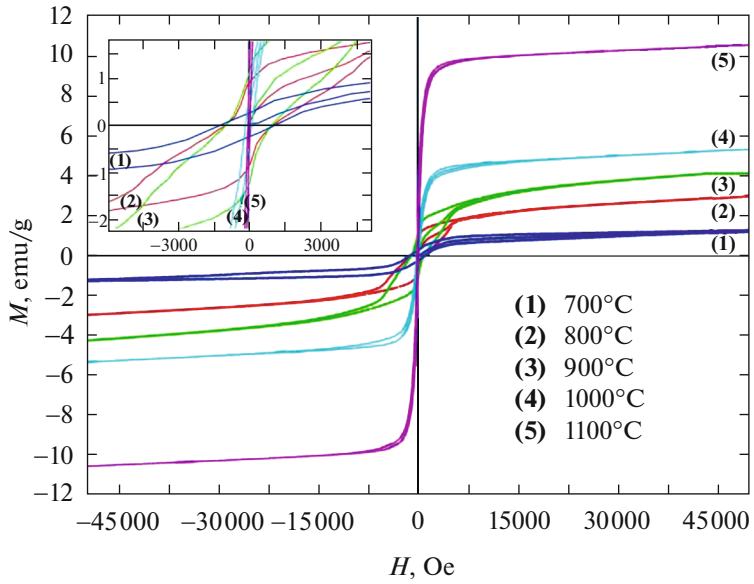

Fig. 2. (Color online) Field dependencies of magnetization (at 300 K) of the samples of magnetic ceramics fabricated by the consolidation of nanostructured hematite at different temperatures. Insert shows the dependence of the coercive force on the SPS temperature.

between sintered particles took place (Figs. 1a, 1a*, 1a**). The presence of external pores ("external porosity") is reflected on the image of the surface cross section of the sample obtained at 900°C (Figs. 1b, 1b*, 1b**). The volume of such pores depends immediately on the degree of bonding between particles and changes in their shapes and packing densities relative to each other.

An important result of the present study consisted in establishing the dependence of magnetic properties of the synthesized ceramic samples on the SPS process temperature. As was shown in [20], even at low-temperature SPS of the α-Fe_2O_3 powder (up to 350°C), the magnetization of composites on its basis was higher and directly proportional to the sintering temperature. Similar regularity was found in the present study. As is seen from a comparison of the field magnetization values of the initial antiferromagnetic hematite (0.8 emu/g) and ceramic samples consolidated on its basis (Fig. 2), this value increases along with the increase of the sintering temperature and is not limited by the value of 10 emu/g (Table 1).

The above effect is to a greater extent explained by changes in the crystalline phase of the initial hematite powder, within which magnetite is formed (Table 1). In other words, a new magnetic phase is formed: Fe_3O_4–α-Fe_2O_3 or γ-Fe_2O_3 [21]. Another reason for this effect could consist in the found growth of the grain (dispersity changes) of the initial hematite during the SPS process (Fig. 1) that affects the system magnetization as well [22, 23]. One must not exclude the possible effect of structural defects in bulk ceramics on its magnetic properties we revealed and described earlier in [24]. In addition, the effect of the direct pulse current on the magnetic susceptibility of the composites under study can be unambiguously stated from the shapes of hysteresis loops (Fig. 2). "Perminvar-like" hysteresis loops are caused by the stabilization of the domain structure—the "perminvar-effect" [25], at which the magnetization direction is stabilized both in domains and in domain walls due to exchange or single-direction magnetic anisotropy. In the case of strong stabilization of magnetization directions in domains and domain walls, the latter are located in deep potential energy wells, and application of an external magnetic field does not result in their shifts. Just upon attainment of the field critical value, the domain boundaries stripping and their shifts development take place. At cyclic field changes, one observes a perminvar-like or double hysteresis loop. Along with the increase of the SPS temperature, such an effect weakens and the coercive force value decreases substantially (from 1130 to 60 Oe) (Table 1).

The studies unambiguously affirm the great potential of SPS technology as a promising method for creating magnetic ceramics in individual and composite systems based on Fe_xO_y.

Bioceramics

The fabrication of bioceramics was investigated on the example of synthesis of calcium monosilicates having a key role in the class of ceramic materials. In particular, the results of our studies were oriented to creating the wollastonite ceramics ($CaSiO_3$), which is an innovative product for medical practice in the last decade [26–28]. The wollastonite ceramics is similar to the bone inorganic matrix with respect to the type of chemical bond, does not have a toxic effect on the organism, and is chemically inert or biologically active at prolonged existence in bioorganic media [29, 30]. That is why it is in high demand in orthopedics, traumatology, stomatology, and other fields of medicine for the recovery, replacement, and reconstruction of

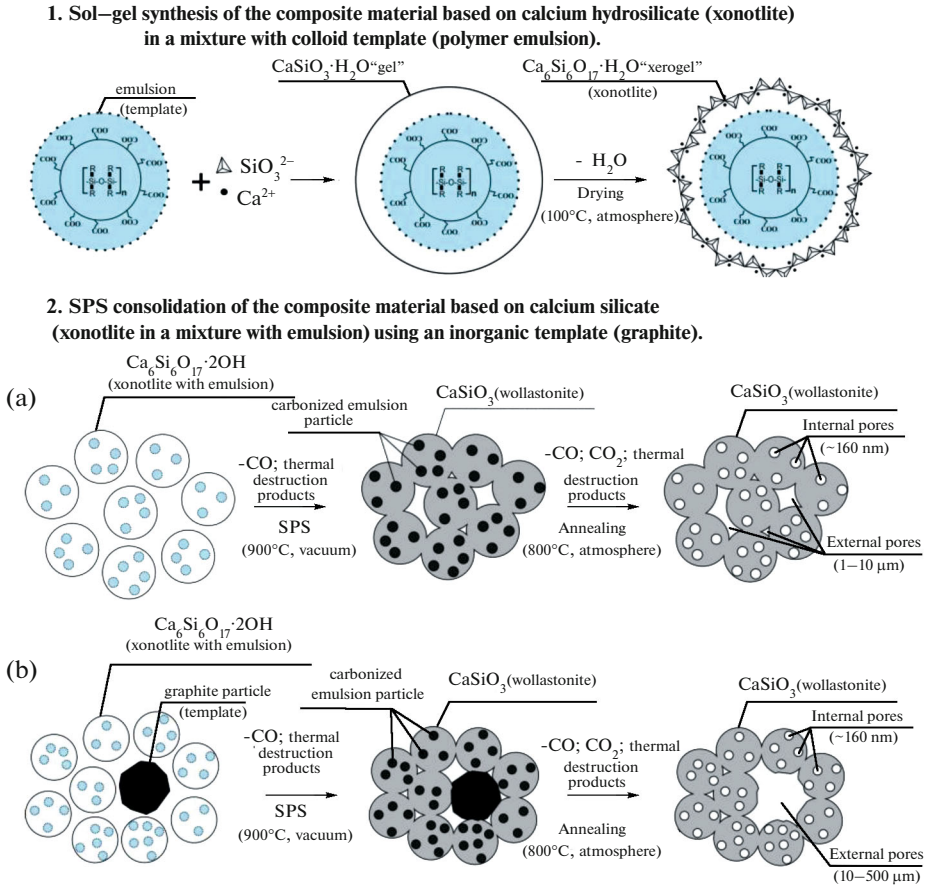

Fig. 3. (Color online) General scheme of two-stage synthesis of biporous ceramic wollastonite using two types of templates.

damaged solid tissues in living organisms. The hierarchical-porous and constructional-strong ceramics comprise a model of a cellular ("spongy" or "spongioid") material constituting a matrix for ingrowth (implantation) of the bone tissue during osteointegration—recovery of the integrity of lost tissue structures in a living organism in the presence of an implant. The intensity of osteointegration depends, first and foremost, on the presence of pores in the implant, in particular, on their size, quantity and degree of interconnection, whereas the minimal pore size is in the range 100–135 μm. In addition, the process of biointegration based on the reproduction of osteogenic cells requires the presence of thin submicron- and nanosized pores commensurable with blood plasma proteins for efficient adsorption of the latter. Also, the strength of such a matrix must be optimal for the homogeneous distribution of the mechanical load between natural and artificial bones to eliminate the probability of excessive destruction of the bone tissue [31, 32]. Thus, it is evident that ceramics characterized with bimodal pore distribution are required for practical medicine purposes. The SPS application in synthesis of the nanostructured ceramics based on bulk wollastonite was demonstrated by a number of authors [33–35], and its composites [36] and bioactive modifications were fabricated [37].

Earlier we performed a successful attempt to create a ceramic wollastonite with a specified set of strength and structural characteristics by means of the SPS method [38]. This work describes the SPS synthesis of a ceramic wollastonite ($CaSiO_3$) on the example of consolidation of the nanostructured wollastonite powder produced by the sol–gel method [39]. The chosen approach is similar to that used in the above described example of synthesis of magnetic ceramics, in which the porous structure of the initial powder to be consolidated is capable of partial preservation after its sintering into a compact compound. In the above work we suggested a method of adjusting the porous structure of $CaSiO_3$ composites produced during SPS synthesis that ensures the formation of a developed porous silicate framework due to the application of a pore-forming component (carbon template) [38]. The method allows the fabrication of materials of predicted porosity from nano- to micrometers, in which the size distribution of the formed pores falls into a certain preset range corresponding to the carbon template size.

A principally new method of structuring the wollastonite ceramics was suggested in the present work. It is based on the fabrication of a ceramic wollastonite of a unique porous structure and comprises an improved variant of the synthesis described above

Table 2. Characteristics of samples of ceramic wollastonite fabricated by sol–gel and SPS methods

	Wollastonite-1	Wollastonite-2	Wollastonite-3
Carbon content, wt %	–	5	25
S_{spec} (BET), m^2/g	3	4	5.7
Fracture strength, MPa	172	117.8	72.5

[38]. However, this new approach is distinguished by the application of a combination of sol–gel and SPS technologies with the simultaneous use of several types of templates, for example, a colloid solution of polymer latex and highly dispersed carbon filler as pore-forming components. The main idea of the method implementation consists of the use of two types of templating agents of different natures, shapes, and sizes, whose introduction is achieved at different stages of the two-stage synthesis (Fig. 3). First (stage 1), a composite material based on calcium hydrosilicate (xonotlite) containing the polymer latex (organic template) is synthesized. During subsequent SPS consolidation of the composite material powder (stage 2a), the formation of nanosized pores of a size of ~160 nm (internal porosity) is provided due to the presence of latex. The introduction of the carbon filler (inorganic template) to the powder to be consolidated (stage 2b) affects the packing of the particles to be sintered and enables one to develop the volume of external pores (external porosity) of the fabricated $CaSiO_3$-ceramics.

This approach has a number of advantages: in particular, it allows preventing the deformation destruction of the internal microstructure (internal porosity) of the wollastonite ceramics occurring at high-temperature (800–1000°C) SPS synthesis. This fact was revealed in our previous work [38], in which the intraporous structure of the wollastonite powder was shown to be unstable to mechanical load and subject to destruction. The method developed in the present work eliminates this problem. The solution consists of the fact that the SPS consolidation is applied to the mentioned nanoporous wollastonite powder, but for to the intermediate product of its synthesis (the composite material obtained at stage 1) by means of sol–gel synthesis. First, a hydrogel of calcium silicate ($CaSiO_3 \cdot H_2O$) is formed in the presence of the polymer latex (template). The silicate gel covers the entire surface of latex particles, forming a solid silicate shell. The microstructure of the preliminarily ground composite substantially changes upon further SPS consolidation (stage 2a). Under intensive heating, the composite powder is actively sintered, and its particles form agglomerates of different sizes. In addition, porous areas (pores) of the interconnected type of a size larger than 1 μm are formed in the structure of the obtained compound. Pores of this type are called "external", determine the "external porosity," and are formed at packing of sintered powder particles [40]. The size and quantity of such pores are determined by the degrees of dispersity and interconnectivity, shape, and density of the packing of particles of the powder to be consolidated. The external porosity parameters are affected by various defects in the solid body. The defect formation is affected by destructive processes emerging under SPS conditions, which may be caused by the following factors: first, thermal decomposition of the material to be sintered under effect of high temperatures and, second, deformation stress under external mechanical load (compacting) on the powder to be consolidated. Despite the above, more important is the fact that deformed latex particles are not burned out during the SPS process: they are just carbonized, preserving the occupied volume in the compound to be sintered. Here, the removal of the latex template to form internal pores is achieved through direct thermal oxidation treatment of the already formed compound (calcining at 800°C in air), i.e., after SPS and, therefore, in the absence of mechanical load forces. The latter is determining in formation of the "internal porosity," which allows preservation of the integrity of the ceramics internal structure.

According to the above scheme, various ceramic samples at carbon template different contents (5 or 25 wt %) were fabricated (Table 2).

In general, the results of low-temperature gas adsorption (BET) and mercury porosimetry indicate the positive dynamics of the increase of the values of specific surface area (Table 2) and pore volume in ceramic samples (Fig. 4a) obtained upon the removal of latex and carbon templates. Depending on the content of the latter (5 or 25 wt %), the volume of external pores increases more than 2- or 3-fold, respectively (Fig. 4a). Here, materials with different pore size distributions (including that of the bimodal type) are formed. As can be seen on the differential dependence of the mercury intrusion (Fig. 4b, curve *3*), the intrusion curve corresponding to 25 wt % of the carbon template additive has two maxima: pores of sizes of 100–500 nm formed due to application of the latex template and those of sizes in the range 1–500 μm due to that of the carbon template.

The presence of the latter pore type in the fabricated ceramics is reflected in SEM images (Fig. 5). It was found that the morphology of the samples surfaces differed in the quantity of large pores (larger than 1 μm), whose number was higher in the case of using the 25 wt % carbon template (Fig. 5b), while they were practically absent upon its low content (Fig. 5a). Despite this, nanosized pores are present in both samples and structured independently of the carbon template quantity (Figs. 5a*, 5b*).

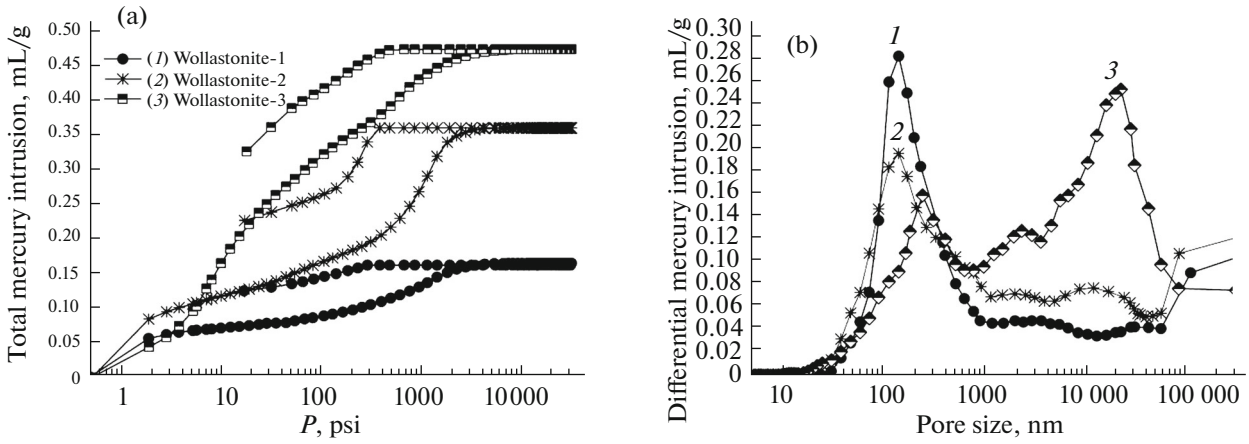

Fig. 4. Differential dependence of the mercury intrusion into the samples of ceramic wollastonite fabricated by SPS: (*1*) without carbon template (sample, Wollastonite-1); (*2*) 5 wt % of carbon template (sample, Wollastonite-2); and (*3*) 25 wt % of carbon template (sample, Wollastonite-3).

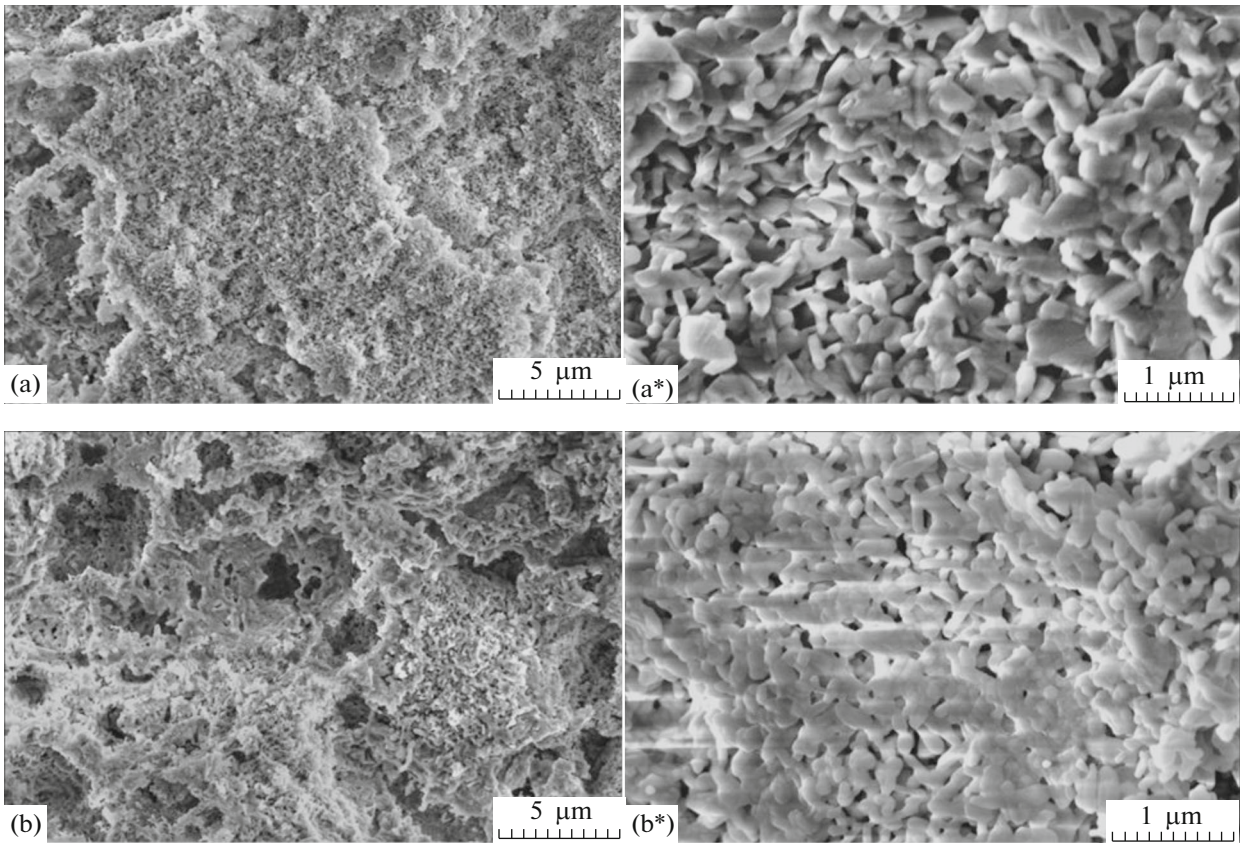

Fig. 5. SEM images of the samples of ceramic wollastonite consolidated by SPS and upon the removal of latex and carbon templates by thermal oxidation treatment at 800°C: (a, a*) 5 wt % of carbon template (sample, Wollastonite-2); (b, b*) 25 wt % of carbon template (sample, Wollastonite-3).

In addition, one should mention that the quality of ceramics of any type is determined, aside from structural characteristics, by strength parameters. The method suggested in the present work is focused on fabrication of the wollastonite ceramics with a unique combination of structural and strength characteristics—a biporous structure (with nano- and microsized pores) of high construction strength (fracture strength from 72.5 to 172 MPa) (Table 2). The biporous structure of the described $CaSiO_3$-based ceramic materials

Fig. 6. (Color online) Samples of ceramic zeolite-based materials fabricated by the SPS synthesis at temperatures from 700 to 1100°C (increment of 100°C).

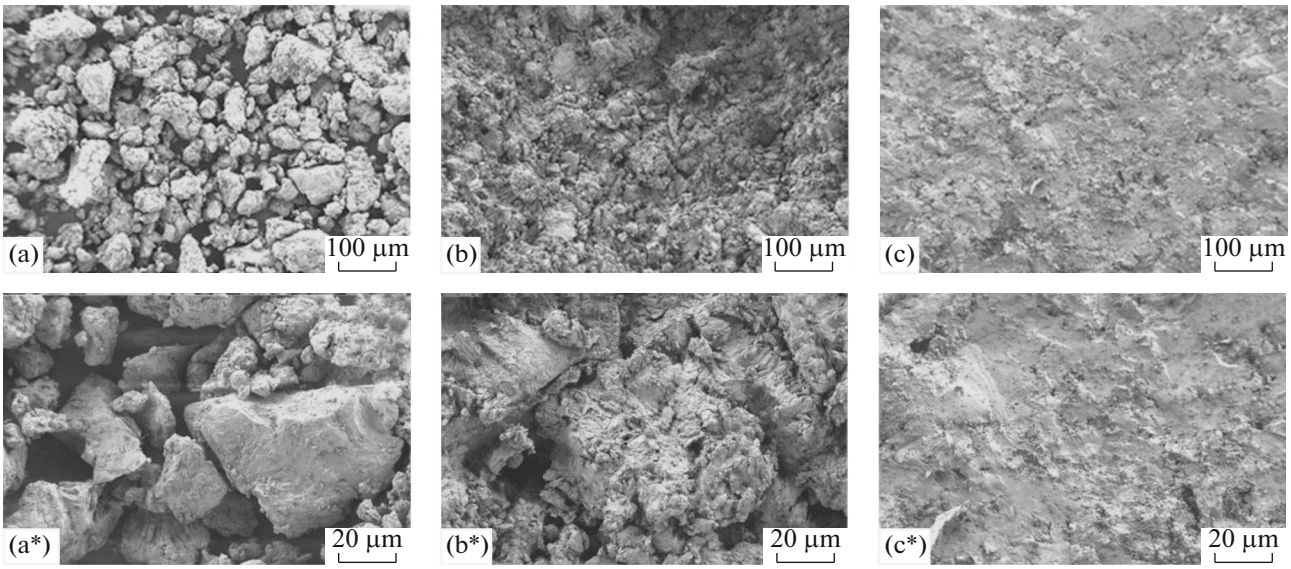

Fig. 7. SEM images of the initial zeolite powder (a, a*) and ceramics samples fabricated by SPS at 800°C (b, b*) and 900°C (c, c*): the sintering pressure is 24.5 MPa.

is similar to the bone tissue texture and able to perform the bone tissue main functions, also at the expense of wollastonite inertness, stability and strength. The fabricated ceramic wollastonite meets the requirements for the class of bioceramic materials [41] and constitutes a promising solution in medical practice.

Nuclear Ceramics

In the safe management of radioactive waste (RAW), a constructive approach would consist of radionuclide immobilization into solid matrices of different types: cement, polymer (including bitumen), glass-forming, and ceramic [42]. With respect to the radionuclide leaching rate, glass-forming and ceramic matrices are the most reliable. Here, from the point of long-term ecological safety, ceramic materials are in the highest demand because of their high chemical and thermal stability [43]. They are extensively used in reliable immobilization of such radionuclides as ^{137}Cs, $^{6\circ}$Co, ^{90}Sr, and ^{235}U. The above radioisotope products in the form of sources of α-, β-, and γ-radiation and nuclear fuel are crucially important for the nuclear industry [44].

Table 3. Features of ceramic samples synthesized by SPS at different temperatures.

T, °C	700	800	900	1000	1100
S_{spec} (BET), m^2/g	17.6	12.6	1.4	0.1	0.1
$\rho_{apparent}$, g/cm^3	1.377	1.420	2.035	2.429	2.429
Mechanical strength (fracture strength), MPa before (after) leaching	22 (6)	27 (8)	123 (43)	503 (366)	489 (313)

In the present work, the possibility of SPS of nuclear ceramics based on natural zeolite (clinoptilolite) containing cesium ions was examined. It was demonstrated that the fabricated zeolite–ceramic compounds of cylindrical shapes (Fig. 6) comprised high-compaction and construction-strong matrices, including the state upon hydrolytic impact (Table 3).

According to the optimal conditions of SPS synthesis of aluminosilicate ceramics in dependence of the required characteristics, at relatively low temperatures (within the range 700–800°C), homogeneous zeolite powder sintering occurs along particle contact boundaries with the preservation of their shape and

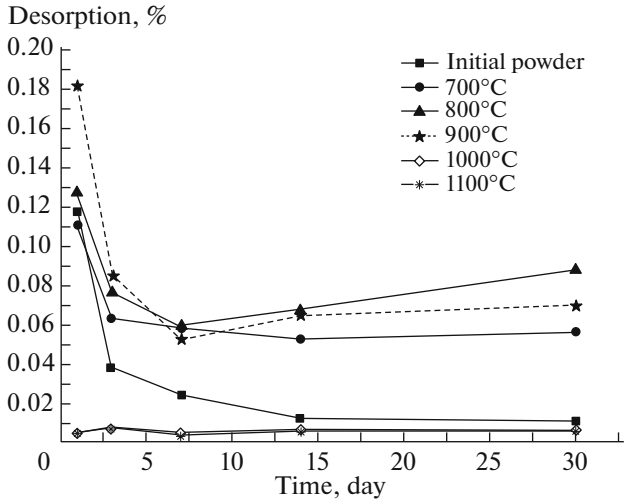

Fig. 8. Rate of leaching of cesium ions from ceramic matrices fabricated by SPS at different temperatures.

size (Figs. 7a, 7a*, 7b, 7b*). Here, ceramic samples have a porous structure of "internal" and "external" types consisting of natural zeolite pores and those formed at particles interaction and packing: the specific surface area is higher than 10 m^2/g (Table 3). High-temperature SPS treatment (above 800°C) was found to destruct the porous structure because of the particle growth, destruction, and melting. A compound of a monolith structure with a mechanical strength (fracture strength) of ~500 MPa is formed (Figs. 7c, 7c*), (Table 3).

The rate of leaching of cesium ions from the samples under study was estimated (Fig. 8). It was shown that ceramic compounds from high-temperature SPS synthesis were characterized with high strength of cesium ions bonding, when compared to that of the initial material powder and low-temperature ceramics. The cesium desorption from such samples is minimal (Fig. 8).

It is worth mentioning that the described approach provides the fabrication of articles of high quality (ceramic matrices), which is achieved by the following factors: (1) low sintering temperature (~1000°C) and minimal duration of the fabrication cycle (<5 min) under a mechanical load of up to 24.5 MPa; (2) it does not require additional stages of raw materials preparation (fractioning, addition of plasticizers, thermal or chemical treatment etc.); (3) a homogeneous distribution of radioactive components in the structure of the formed ceramic matrix is attained though the use of aluminosilicate raw materials (zeolites) characterized with a homogeneous porous structure and, as a result, high fraction of free volume; (4) it is also possible to manufacture final products in the form of capsules of specified standard sizes (from 1.0 to 100.0 mm); and (5) application of the compacted glass bulk characterized with abnormally low rates of leaching of ^{137}Cs by water ($<10^{-6}$–10^{-7} g/cm^2 day), high construction strength (fracture strength ~500 MPa), and a cesium mass fraction of ~20%.

To sum up, it is evident that application of the SPS technology at high temperatures can be recommended for the consolidation of powder materials containing hazardous radionuclides (for example, spent sorbents saturated with radioactive cesium) into hard compounds suitable for safe long-term storage (disposal). In addition, even more promising application is related to producing ionizing radiation sources containing zeolite glass ceramics with immobilized radionuclides with a precise specific activity as an active base (filler) [45].

CONCLUSIONS

The present study was focused on studies of the applicability of the innovative SPS technology and its possible combinations with other inorganic synthesis methods (for example, the sol–gel method) in the fabrication of multifunctional ceramics for various practical purposes.

A magnetic ceramic material for various applications in electrical engineering was successfully synthesized by the SPS method, in particular, on the basis of the nanostructured hematite powder obtained using the sol–gel technology. It has been established that phase composition and microstructure of high-temperature magnetic ceramics based on an individual α-Fe_2O_3 (hematite) and an α-Fe_2O_3–Fe_3O_4 composite (hematite–magnetite) are heterogeneous. The crystalline α-Fe_2O_3 is unstable and becomes partially reduced in the spark plasma flow to Fe_3O_4 above 900°C. As was found in microscopy studies, solid-phase processes were activated under the above sintering conditions, whereas upon the temperature increase one observes a significant grain growth and particles reorientation and deformation, which results in the destruction of the material internal and external structures. The ceramic strength reaches 249 MPa at a specific surface area of 0.7–0.1 m^2/g. The ceramic composites magnetic properties have been studied, and it has been shown that the value of magnetization of the antiferromagnetic hematite powder (0.8 emu/g) changes significantly upon high-temperature SPS treatment, increases along with the sintering temperature increase, and attains 10.2 emu/g at 1100°C (a more than tenfold increase).

An original method of fabricating high-quality bioceramics based on the combined application of sol–gel and SPS technologies has been developed on the example of synthesis of a ceramic wollastonite characterized with a unique set of structural and strength characteristics: porous structure with bimodal pore size distribution (100–500 nm and 1–500 μm), high construction strength (from 72.5 to 172 MPa). Creating a biporous silicate framework in the ceramic compound was provided through the additional use of templates of different nature. It has been demon-

strated that a colloid template (polymer latex) introduced at the sol–gel synthesis stage is resistant to deformation stress emerging upon the mechanical load during the SPS synthesis, which promotes the formation of defect-free nanosized pores (internal porosity) in the compound bulk after the latex thermal. The efficiency of using an inorganic template (carbon filler) to obtain micrometer-sized pores (external porosity) has been revealed. The fabricated ceramics are characterized with the presence of a biporous structure similar to the texture of the bone tissue and capable of achieving its basic functions, also due to inertness, stability, and strength of wollastonite. Bioceramics of this type constitute a promising solution in medical practice.

Unique studies of the SPS synthesis of high-compaction ceramic matrices applicable for immobilization of high-energy radionuclides have been performed. Ceramic samples in the form of the compacted glass characterized with abnormally low rates of leaching of cesium ions by water ($<10^{-6}$–10^{-7} g/cm^2 day), high construction strength (fracture strength 500 MPa), and a cesium mass fraction of ~20% have been fabricated. The uniqueness of the suggested technological approach has a background of advantages over conventional methods: in particular, a high quality of manufactured articles is achieved through a low sintering temperature (maximum 1100°C) and minimal fabrication cycle duration (maximum 5 min); absence of an additional stage of raw materials preparation (fractioning, addition of plasticizers, thermal and chemical treatment etc.); ensuring homogeneity of radioactive components distribution in the structure of the formed ceramic matrix; manufacturing finished molded products of specified standard sizes; and the possibility of precise doping of the initial materials with radioactive components (precise specific activity) with acceptable dispersion no higher than ±5%.

The studies confirm the high potential of SPS technology as a promising approach in creating a new type of ceramic materials for extensive practical applications, including those having no worldwide analogs. The results are of scientific and practical value both for understanding specific features of the SPS process in formation of new types of ceramics and for creating commercial products on their basis. The innovativeness of the SPS technology opens up for researchers wide prospects in the formation of fundamentals and a gain of theoretical knowledge of synthesis of new nanostructures characterized with unique compositions and functional properties, which makes it possible to develop various original methods of synthesis of novel materials for efficient solutions of concrete technological problems.

ACKNOWLEDGMENTS

This study was partially supported by the Russian Science Foundation (project no. 14-13-00135 (Nuclear Ceramics part)) and Russian Foundation for Basic Research (project no. 14-03-00096 (Magnetic Ceramics part) and by grant for young scientists from the President of the Russian Federation (project MK-177.2017.3 (Bioceramics part)).

REFERENCES

1. E. G. Grigor'ev and B. A. Kalin, *Electric Pulse Technology Forming of Material from Powders,* The School-Book (Mosk. Inzh. Fiz. Inst., Moscow, 2008) [in Russian].
2. R. Orru, R. Licheri, A. M. Locci, A. Cincotti, and G. Cao, "Consolidation/synthesis of materials by electric current activated/assisted sintering," Mater. Sci. Eng. R **63**, 127–287 (2009).
3. Z. A. Munir and D. V. Quach, "Electric current activation of sintering: a review of the pulsed electric current sintering process," J. Am. Ceram. Soc. **94**, 1–19 (2011).
4. M. Tokita, "Trends in advanced sPS spark plasma sintering systems and technology," J. Soc. Powder Technol. Jpn. **30**, 790–794 (1993).
5. V. Mamedov, "Spark plasma sintering as advanced PM sintering method," Powder Metall. **45**, 322–328 (2002).
6. O. L. Khasanov, E. S. Dvilis, Z. G. Bikbaeva, *Methods of Compaction and Consolidation of Nanostructured Materials and Products* (Tomsk. Politekh. Univ., Tomsk, 2008) [in Russian].
7. *Nanoscale Magnetic Materials and Applications,* Ed. by P. Liu, E. Fullerton, O. Gutfleisch, and D. J. Sellmyer (Springer, New York, 2009).
8. E. K. Papynov, I. A. Tkachenko, V. Yu. Maiorov, A. A. Kvach, A. S. Kuchma, A. S. Portnyagin, A. N. Dran'kov, O. O. Shichalin, T. A. Kaidalova, T. A. Sokol'nitskaya, V. A. Avramenko, "Template synthesis of porous iron oxides with magnetic and catalytic properties," Fundam. Issled., No. 11 (4), 816–821 (2014).
9. H. H. Wang, X. R. Li, G. Q. Fei, and J. Mou, "Synthesis, morphology and reology of core-shell silicone acrylic emulsion stabilized with polymerisable surfactant," eXPRESS Pol. Lett. **4**, 670–680 (2010).
10. E. K. Papynov, V. Yu. Mayorov, M. S. Palamarchuk, and V. A. Avramenko, "Peculiarities of formation of phase composition, porous structure, and catalytic properties of tungsten oxide-based macroporous materials fabricated by sol-gel synthesis," Mater. Res. A **88**, 42–51 (2014).
11. D. Breck, *Zeolite Molecular Sieves* (Wiley, New York, 1974).
12. K. H. J. Buschow and F. R. de Boer, *Physics of Magnetism and Magnetic Materials* (Springer, New York, 2003), p. 182.
13. *Modern Techniques for Characterizing Magnetic Materials,* Ed. by Yimei Zhu (Springer, New York, 2005), p. 583. doi 10.1007/b101202
14. *Nanostructured Magnetic Materials and their Applications, Series II: Mathematics, Physics and Chemistry,* Ed. by B. Aktaş, L. R. Tagirov, and F. Mikailov (Springer, Netherlands, 2004), p. 443. doi 10.1007/978-1-4020-2200-5
15. Chunlong Fei, Yue Zhang, Zhi Yang, Yong Liu, Rui Xiong, Jing Shi, and Xuefeng Ruan, "Synthesis and magnetic properties of hard magnetic ($CoFe_2O_4$)-soft

magnetic (Fe_3O_4) nano-composite ceramics by SPS technology," J. Magn. Magn. Mater. **323**, 1811–1816 (2011).

16. W. Chen, U. Anselmi-Tamburini, J. E. Garay, J. R. Groza, and Z. A. Munir, "Fundamental investigations on the spark plasma sintering/Synthesis process I. Effect of dc pulsing on reactivity," Mater. Sci. Eng. A **394**, 132–138 (2005).
17. Zhoungwu Wang and S. K. Saxena, "Pressure induced phase transformations in nanocrystaline maghemite (γ-Fe_2O_3)," Solid State Commun. **123**, 195–200 (2002).
18. M. Murakami, K. Hirose, Sh. Ono, T. Tsuchiya, M. Isshiki, and T. Watanuki, "High pressure and high temperature phase transitions of FeO," Phys. Earth Planet. Inter. **146**, 273–282 (2004).
19. Z. Wang and S. K. Saxena, "Pressure induced phase transformations in nanocrystaline maghemite (γ- Fe_2O_3)," Solid State Commun. **123**, 195–200 (2002).
20. P. Saravanan, Jen-Hwa Hsu, D. Sivaprahasam, and S. V. Kamat, "Structural and magnetic properties of γ- Fe_2O_3 nanostructured compacts processed by spark plasma sintering," J. Magn. Magn. Mater. **346**, 175–177 (2013).
21. A. Bertrand, J. Carreaud, G. Delaizir, J.-R. Duclere, M. Colas, J. Cornette, M. Vandenhende, V. Couderc, and Ph. Thomas, "A comprehensive study of the carbon contamination in tellurite glasses and glass-ceramics sintered by spark plasma sintering (SPS)," J. Am. Ceram. Soc. **97**, 163–172 (2013). doi 10.1111/jace.12657
22. C. J. Goss, "Saturation magnetisation, coercivity and lattice parameter changes in the system Fe_3O_4–γ-Fe_2O_3, and their relationship to structure," Phys. Chem. Miner. **16**, 164–171 (1988).
23. A. E. Berkowitz, W. J. Schuele, and P. J. Flanders, J. Appl. Phys. **39**, 1261–1263 (1968).
24. E. K. Papynov, I. A. Tkachenko, A. S. Portnyagin, E. B. Modin, and V. A. Avramenko, "Fabrication of magnetic ceramic materials based on nanostructured hematite powder by spark plasma sintering," ARPN J. Eng. Appl. Sci. **11**, 5864–5870 (2016).
25. J. Stöhr and H. Ch. Siegmann, *Magnetism* (Springer, Berlin, Heidelberg, 2006), p. 822. doi 10.1007/978-3-540-30283-4
26. J. M. Sautier, T. Kokubo, T. Ohtsuki, J. R. Nefussi, H. Boulekbache, M. Oboeuf, S. Loty, C. Loty, and N. Forest, "Bioactive glass-ceramic containing crystalline apatite and wollastonite initiates biomineralization in bone cell cultures," Cal. Tiss. Inter. **55**, 458–466 (1994).
27. S. A. Saadaldina and A. S. Rizkalla, "Synthesis and characterization of wollastonite glass-ceramics for dental implant applications," Dent. Mater. **30**, 364–371 (2014).
28. V. A. Dubok, "Bioceramics – yesterday, today, tomorrow," Powder Metall. Metal. Ceram. **39**, 381–394 (2000).
29. Y.-H. Yun, S.-D. Yun, H.-R. Park, Y.-K. Lee, and Y.-N. Youn, "Preparation of β-wollastonite glass-ceramics," J. Mater. Synth. Process **10**, 205–209 (2002).
30. G. M. Azarov, E. V. Maiorova, M. A. Oborina, and A. V. Belyakov, "Wollastonite raw materials and their applications (a review)," Glas. Ceram. **52**, 237–240 (1995).
31. Q. Huang, L. Wang, and J. Wang, "Mechanical properties of artificial materials for bone repair," J. Shanghai Jiaot. Univ. (Sci.) **19**, 675–680 (2014).
32. J. A. Juhasz and S. M. Best, "Bioactive ceramics: processing, structures and properties," J. Mater. Sci. **47**, 610–624 (2012).
33. Q. Z. Chen, J. L. Xu, L. G. Yu, X. Y. Fang, and K. A. Khor, "Spark plasma sintering of sol-gel derived 45A5 Bioglass®-ceramics: mechanical properties and biocompatibility evaluation," Mater. Sci. Eng. C **32**, 494–502 (2012).
34. Y. W. Gu, N. H. Loh, K. A. Khor, S. B. Tor, and P. Cheang, "Spark plasma sintering of hydroxyapatite powders," Biomaterials **23**, 37–43 (2002).
35. X. Wan, A. Hu, M. Li, C. Chang, and D. Mao, "Perfomance of $CaSiO_3$ ceramic sintered by spark plasma sintering," Mater. Char. **59**, 256–260 (2008).
36. L. Long, F. Zhang, L. Chen, L. Chen, and J. Chang, "Preparation and properties of β-$CaSiO_3$/ZrO_2 (3Y) nanocomposites," J. Eur. Ceram. Soc. **28**, 2883–2887 (2008).
37. L. H. Long, L. D. Chen, S. Q. Bai, J. Chang, and K. L. Lin, "Preparation of dense β-$CaSiO_3$ ceramic with high mechanical strength and hap formation ability in simulated body fluid," J. Eur. Ceram. Soc. **26**, 1701–1706 (2006).
38. E. K. Papynov, V. Yu. Mayorov, A. S. Portnyagin, O. O. Shichalin, S. P. Kobylyakov, T. A. Kaidalova, A. V. Nepomnyashiy, T. A. Sokol'nitskaya, Yu. L. Zub, and V. A. Avramenko, "Application of carbonaceous template for porous structure control of ceramic composites based on synthetic wollastonite obtained via spark plasma sintering," Ceram. Int. **41**, 1171–1176 (2015).
39. E. K. Papynov, V. Yu. Maiorov, E. B. Modin, E. V. Kaplun, T. A. Sokol'nitskaya, and V. A. Avramenko, "Template synthesis of porous calcium monosilicates using siloxane-acrylate latexes," Fundam. Issled., No. 12, 505–510 (2015).
40. L. H. Long, L. D. Chen, S. Q. Bai, J. Chang, and K. L. Lin, "Preparation of dense β-$CaSiO_3$ ceramic with high mechanical strength and hap formation ability in simulated body fluid," J. Eur. Ceram. Soc. **26**, 1701–1706 (2006).
41. I. G. Maryasev, L. M. Mikhailovskaya, L. D. Bocharov, E. F. Chaika, D. A. Tereshchenko, A. A. Platonov, and G. R. Platonova, "Pores: their classification and role in actual refractory material structures," Refract. Ind. Ceram. **52**, 202–211 (2011).
42. V. I. Bulatov, T. A. Kalyuzhnaya, L. I. Kuzubova, and O. L. Lavrik, *Radioactive wastes Environmental Problems and Management, Bibliographic Review, Part 2: Radioactive Waste Storage* (GPNTB SO RAN, Novosibirsk, 1998) [in Russian].
43. P. Trocellier and R. Delmas, "Chemical durability of zircon," Nucl. Instrum. Methods Phys. Res. Bull. **181**, 408–412 (2001).
44. A. I. Zhiganov, V. V. Guzeev, and G. G. Andreev, *Technology of Uranium Dioxide for Ceramic Nuclear Fuel* (STT, Tomsk, 2002) [in Russian].
45. A. S. Aloi, S. V. Baranov, and M. V. Logunov, *Gamma Ray Sources with Cesium 137 (Properties, Production, Application)* (Mayak, Ozersk, 2013) [in Russian].

Translated by D. Marinin